



OPEN ACCESS

EDITED BY

Xinjiang Hu,
Central South University Forestry and
Technology, China

REVIEWED BY

Zhujian Huang,
South China Agricultural University,
China
Ling Luo,
Sichuan Agricultural University, China

*CORRESPONDENCE

Pufeng Qin,
✉ qinpufeng@126.com

SPECIALTY SECTION

This article was submitted to Water and
Wastewater Management,
a section of the journal
Frontiers in Environmental Science

RECEIVED 02 November 2022

ACCEPTED 05 December 2022

PUBLISHED 23 January 2023

CITATION

Dai Z, Qin T, Bai C, Wu Z, Gao Y and
Qin P (2023), Simultaneous treatment of
phosphorus and fluoride wastewater
using acid-modified iron-loaded
electrode capacitive deionization:
Preparation and performance.
Front. Environ. Sci. 10:1087231.
doi: 10.3389/fenvs.2022.1087231

COPYRIGHT

© 2023 Dai, Qin, Bai, Wu, Gao and Qin.
This is an open-access article
distributed under the terms of the
[Creative Commons Attribution License
\(CC BY\)](https://creativecommons.org/licenses/by/4.0/). The use, distribution or
reproduction in other forums is
permitted, provided the original
author(s) and the copyright owner(s) are
credited and that the original
publication in this journal is cited, in
accordance with accepted academic
practice. No use, distribution or
reproduction is permitted which does
not comply with these terms.

Simultaneous treatment of phosphorus and fluoride wastewater using acid-modified iron-loaded electrode capacitive deionization: Preparation and performance

Zhijian Dai, Tian Qin, Chengke Bai, Zhibin Wu, Ya Gao and Pufeng Qin*

College of Resources and Environment, Hunan Agricultural University, Changsha, China

Here, capacitive deionization technology (CDI) using modified activated carbon fiber felt (ACF) electrodes was proposed to provide a new strategy for the challenge of simultaneous phosphorus and fluoride wastewater treatment. The acid-modified iron-loaded ACF (A@Fe-ACF) was obtained by modifying ACF through a two-step impregnation method. After the modification, the oxygen-containing functional groups on ACF increased and provided more adsorption sites. The electron transfer efficiency on the A@Fe-ACF was increased by introducing Fe and synergistically promoted the adsorption of phosphorus and fluorine. Results showed that the removal efficiencies of total phosphorus (TP) and total fluorine (TF) in wastewater reached 89.4% and 85% under optimal conditions (voltage intensity 1.5 V, pH 7, plate spacing 1 cm), while the adsorption mechanism of phosphorus and fluorine was dominated by chemical adsorption. Meanwhile, A@Fe-ACF electrode has good recyclability and stability after five cycles.

KEYWORDS

capacitive deionization, acid-modified, iron-loaded, phosphorus and fluoride wastewater, simultaneous treatment

1 Introduction

With the rapid development of the agricultural economy, water pollution caused by the discharge of phosphorus chemical sewage was increasingly severe (Xia et al., 2021). The phenomenon of excessive phosphorus and fluorine produced in the production process of phosphorus compound fertilizer has received significant attention. The characteristics of this type of wastewater are acidic, and the primary pollutants exist in various forms, such as F^- , SiF_6^{2-} , PO_4^{3-} , $H_2PO_4^-$, and HPO_4^{2-} , posing serious harm to ecology and human health (Gouider et al., 2010). The neutralization precipitation process is the primary strategy to treat phosphorus and fluoride wastewater, while fluoride and phosphate ions can be precipitated

and separated from the water body (Al-Harabsheh et al., 2014; Wang et al., 2020). However, there are problems with the high cost and the large amount of sludge caused by adding a large amount of neutralizing reagents. It is challenging to realize the requirements of water purification while considering the economy. Current treatment technology mainly focuses on phosphorus or fluorine removal alone, but the efficient process for simultaneous removal of phosphorus and fluoride still has a large exploration potential. In light of this, developing a clean, efficient, and sustainable technology for phosphorus and fluoride removal from wastewater is significant.

Capacitive deionization technology has been widely used as a promising electrochemical technology in the past decade due to low energy consumption, easy electrode regeneration, and no secondary pollution (Ayranci and Conway, 2001; Kalfa et al., 2020; Chai et al., 2021). The electric field is applied to the electrode to form an electric double layer at the electrode/solution interface, then the charged ions in the solution are enriched and concentrated at the electrode interface, thereby realizing the removal of pollutant targets. The electrode material is a crucial part of CDI which significantly influences this process. Among many reported electrode materials, activated carbon fiber felt (ACF), as a low-cost electrode material with high specific surface area, rich pore structure, and stable electrochemical performance, was widely used in the CDI treatment of wastewater (Foo and Hameed, 2009; Chen et al., 2015). The CDI process based on the ACF electrodes has achieved good results in treating phosphorus or fluoride-containing wastewater, and the effect of CDI could be further improved by modifying ACF (Zhang et al., 2020; Martinez-Vargas et al., 2021). In addition, CDI also played a vital role in composite wastewater containing phosphorus or fluoride (Gaikwad and Balomajumder, 2017). Optimized carbon-based electrodes will provide more adsorption sites, which creates opportunities to remove multiple contaminants (Kalfa et al., 2020). Although it has promising prospects in complex wastewater, the study of the simultaneous treatment of phosphorus and fluoride in wastewater through CDI still needs to be completed. Considering above these, treating phosphorus and fluoride in wastewater simultaneously based on CDI using the ACF electrode may be a meaningful and feasible solution.

To further improve the ACF electrode performance, it was modified by acid treatment and iron salt impregnation in our work for the simultaneous treatment of phosphorus and fluoride wastewater. Fe was introduced to enhance the binding with pollutants, reduce the resistance of ACF, and improve the electrochemical performance of electrode. After the electrodes were prepared, a series of characterizations were carried out. The influence of critical factors on the removal efficiency of phosphorus and fluoride wastewater was systematic explored to evaluate the potential in practical application. The mechanism of phosphorus and fluoride removal was also discussed. Finally, the stability and reusability of the modified ACF electrodes were investigated. This work aims to provide a new idea for the simultaneous treatment of phosphorus and fluoride wastewater.

2 Experiment section

2.1 Wastewater and reagents

The phosphorus and fluoride wastewater used in this experiment was collected from the phosphate fertilizer factory (Zhuzhou, China), and the detailed information are: pH 3.53, 82.7 mg/L TF, 121.2 mg/L TP, 112.5 mg/L COD, 1800 mg/L SO_4^{2-} , 45 mg/L $\text{NH}_3\text{-N}$, and 3,320 $\mu\text{s/cm}$ conductivity. All experiments were conducted using ultrapure water (UPH, 18.25 $\text{M}\Omega\text{-cm}$). The pH of the wastewater was adjusted by 0.1 mM NaOH solution.

2.2 Preparation of modified electrode

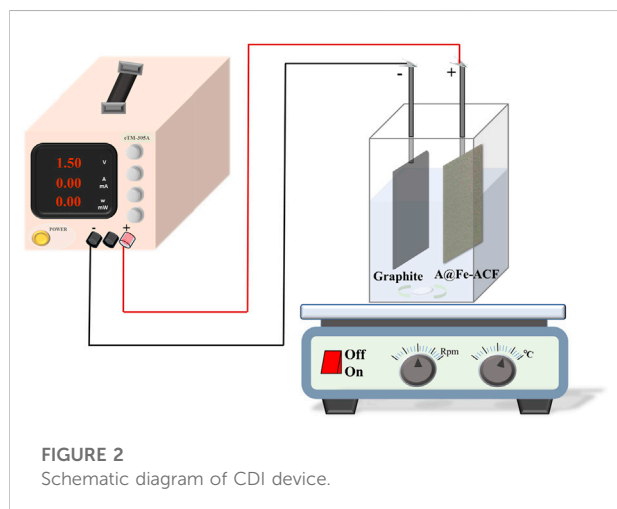
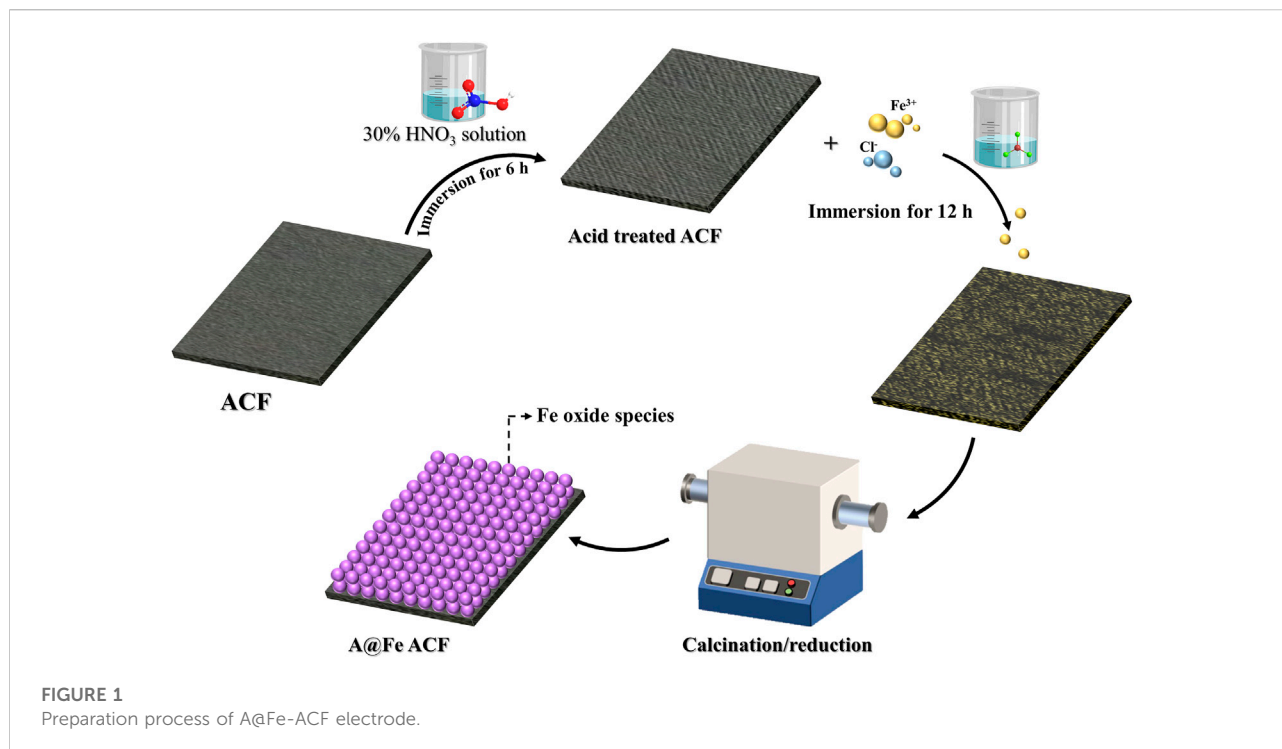
The electrode preparation process was shown in Figure 1. The commercial ACF was cut into 5×10 cm squares, placed in a beaker, boiled with boiling water for 2 h, and soaked in absolute ethanol for 2 h to remove ash impurities in the ACF. Then, the ACF was soaked in 30% HNO_3 solution for 6 h, washed with ultrapure water until the pH reached neutrality, and dried. Next, the acid-treated ACF was immersed in 200 ml of FeCl_3 solution (0%–3%) for 12 h. After taking it out to dry, the ACF was put in a tube furnace for calcination at different temperatures under an N_2 atmosphere for 4 h to obtain the A@Fe-ACF electrode.

2.3 Electrode characterization

The properties of the prepared ACF electrodes were characterized using different analytical techniques, including X-ray diffraction (XRD, Ultima IV, Japan), Scanning electron microscopy (SEM, Hitachi S4800, Japan), X-ray photoelectron spectroscopy (XPS, Thermo ESCALAB 250XI, United States), Fourier transform infrared absorption spectroscopy (FTIR, Nicolet iN10, United States), surface area and pore size analyzer (BET, ASAP2460, United States), and electrochemical impedance spectroscopy measurements (EIS, CHI 660E, China).

2.4 Experiment procedure

The CDI process was performed in a special acrylic cuboid reactor ($L = 10$ cm, $W = 5$ cm, $H = 12$ cm), with A@Fe-ACF as the anode attached to a stainless-steel plate and graphite plate as the cathode (Figure 2; Supplementary Figure S1). The electrodes are connected to a direct current (DC) regulated power supply (MESTEK DP3030) and maintained at a constant distance. After applying a voltage to the electrodes to initiate the reaction, key parameters such as voltage intensity, initial pH, plate spacing, and phosphorus and fluoride (P/F) ratio on phosphorus and fluoride removal efficiency were investigated by a conventional



parametric approach. At preselected time intervals, the extracted solutions were transferred to 5 ml sampling tubes and analyzed uniformly.

2.5 Analysis methods

The concentration changes of total phosphorus (TP) and total fluorine (TF) were used to represent the removal efficiency of phosphorus and fluorine. Molybdenum antimony anti-

spectrophotometry was used to determine the concentration of total phosphorus. The ion-selective electrode method was used to determine the TF concentration (the indicator electrode was a fluoride ion-selective electrode, and the reference electrode was a saturated calomel electrode).

2.6 Statistics analysis

Data used in this study were entered in Excel, and all data were tested for normality (Shapiro-Wilk test) and homogeneity (Levene test) before analysis, and Duncan multiple comparisons were performed on the data means. TP and TF removal efficiency under different conditions were analyzed by one-way ANOVA. All data were statistically analyzed using IBM SPSS Statistics 23.0 software.

3 Results and discussion

3.1 Characteristics of A@Fe-ACF

The morphologies of ACF before and after modification are shown in Figure 3. The initial ACF surface was smooth and flat (Figure 3A), and it became rough after HNO₃ modification (Figure 3B) due to the strong oxidizing property of HNO₃ corroding the ACF surface. The surface morphology of ACF was changed after acid treatment, and the pore structure was

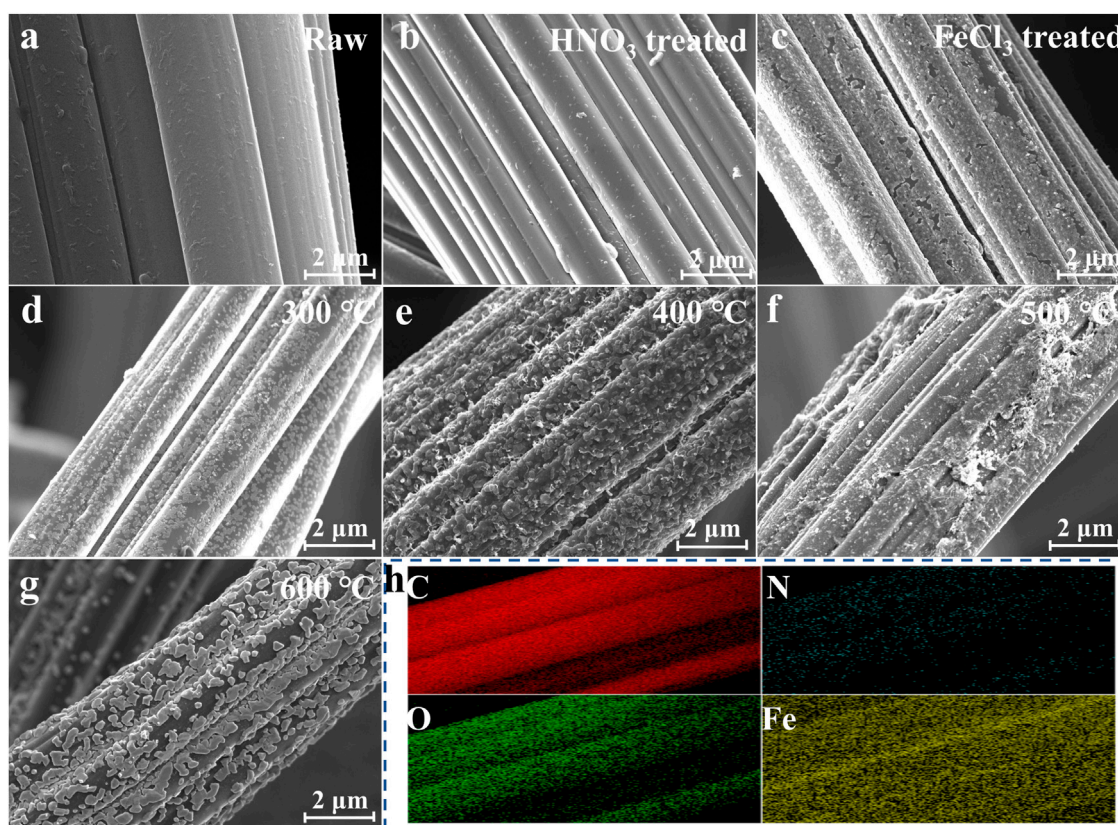


FIGURE 3

SEM of A@Fe-ACF under different calcination temperature: (A) Raw. (B) ACF treated by HNO_3 . (C) ACF treated by FeCl_3 . (D) 300°C . (E) 400°C . (F) 500°C . (G) 600°C . (H) Element mapping of A@Fe-ACF.

increased, which significantly increased the specific surface area of ACF (Figure 4A). Furthermore, the acid-treated ACF could provide more loading sites for Fe, conducive to the tighter bonding between the loading metal and the carrier. It can be seen that the iron oxide was covered on the ACF in a sheet shape when the iron loading modification was carried out alone (Figure 3C). The smooth carbon fiber surface does not provide an excellent binding point for the Fe element and will lead to the iron oxide difficult to bonded on the ACF and is easy to fall off. When ACF was treated with acid and modified with Fe loading, it could be observed that Fe oxides were tightly bound on ACF in irregular granular form compared with the modification of Fe alone (Figures 3D–H). Although Fe loading leads to a slight decrease in the specific surface area (Figure 4A), the synergistic effect of Fe oxides has further improved the TP and TF removal. The calcination temperature is another key factor affecting the CDI performance of A@Fe-ACF, as the adsorption efficiency gradually increased with the temperature. However, the removal efficiency of TP and TF decreased when the temperature was higher than 400°C (Supplementary Figures S2A, 2B). It can be seen from SEM that the Fe oxide on the surface of ACF is evenly

distributed at 400°C , while the Fe oxide begins to sinter, and the load area becomes smaller when the temperature increases to 500°C – 600°C (Figures 3E, F), thus affecting the CDI efficiency of A@Fe-ACF. In addition, the load of Fe is also an essential factor. The introduction of iron improved the adsorption efficiency of phosphorus and fluorine in wastewater, while the adsorption capacity also increased significantly with the loading concentration (Supplementary Figure S2C). However, the higher loading concentration would lead to Fe oxide blocking pores and inhibit the effect of CDI process. Therefore, 2% Fe loading concentration and the 400°C calcination temperature were the optimal conditions for A@Fe-ACF. The electrochemical properties of the electrodes were compared using EIS (Supplementary Figure S3), and it can be seen that the transfer resistance of the ACF decreases significantly with Fe loading. The presence of Fe accelerated the electron transfer efficiency and improved the conductivity of the electrode, which facilitated the capacitive deionization process.

Figure 4B showed the FTIR images under different modification conditions. The characteristic peak at $3,460\text{ cm}^{-1}$ is the stretching vibration peak of -OH, and the absorption peak

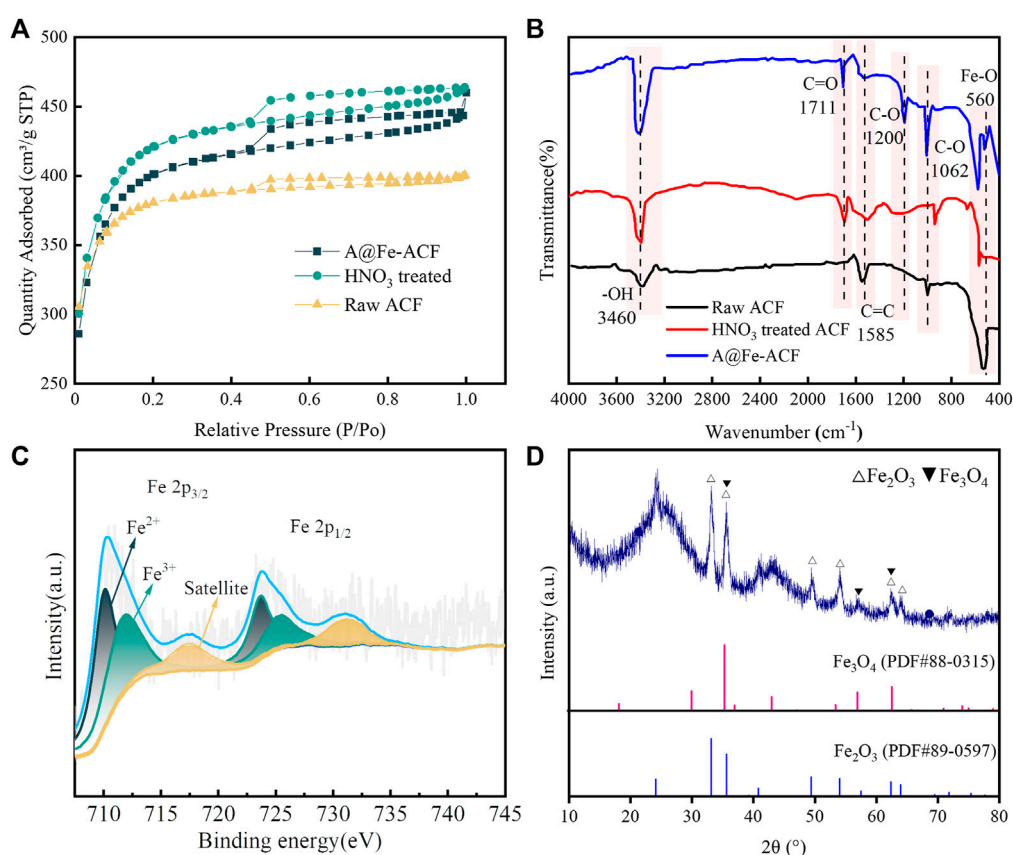


FIGURE 4

(A) N₂-adsorption isotherms of electrodes with different modification. (B) FTIR of electrodes with different modifications. (C) XPS spectrum of A@Fe-ACF-400. (D) The XRD spectrum of A@Fe-ACF-400.

here is significantly enhanced after modification, indicating that the hydrophilicity of the material has been improved. The new peak at 1711 cm⁻¹ may be the characteristic peak of C=O bond stretching vibration in the carboxylic acid group, representing the introduction of oxygen-containing functional groups after acid modification (Wu et al., 2015). The peak at 1,630 cm⁻¹ represents the backbone vibration of C=C, where the intensity gradually decreased with ACF modification. This phenomenon might be caused by the high temperature brought by the heat treatment (Wang et al., 1994; Georgakopoulos, 2003). The enhancement of the C-O bond at 1,200 cm⁻¹ and 1,062 cm⁻¹ could be attributed to the production of more abundant oxygen-containing groups (Meng et al., 2018). Moreover, the metal oxide peak at 560 cm⁻¹ is Fe-O (Verma et al., 2021), which further proved that Fe was efficiently loaded on the ACF surface.

From XPS analysis in Figure 4C, it could be observed that Fe in A@Fe-ACF-400 exists as Fe²⁺ and Fe³⁺, which could be attributed to the introduction of oxygen-containing functional groups promoted the redox on the electrode surface (Ren et al., 2020). The cycling of Fe²⁺/Fe³⁺ increased the current efficiency, thereby indirectly improving the effect of the CDI process (Wang

et al., 2021). The iron element in A@Fe-ACF-400 mainly existed in Fe₂O₃ and Fe₃O₄ (shown in Figure 4D). The characteristics of Fe oxides could enhance the electron transfer in the electric field and improve the efficiency of electro adsorption to remove phosphorus and fluorine ions (Song et al., 2019).

3.2 Effect of key factors on CDI performance

Voltage intensity played a crucial role in the CDI process. It can be seen from Figures 5A, B that the removal of TP and TF showed a trend of first high and then low with the increase of voltage. When the voltage was 1.5 V, the removal of TP and TF reached 89.4% and 85%. The increase in voltage drives a higher current and establishes a steady-state faster, then the increase in electron mobility promotes the accumulation and adsorption of contaminant ions in the electric double-layer (Chai et al., 2020; Lin et al., 2022). However, the removal efficiency dropped to 83% and 78% when the voltage intensity was increased to 2 V. That is the excessively high voltage aggravating the hydrogen evolution

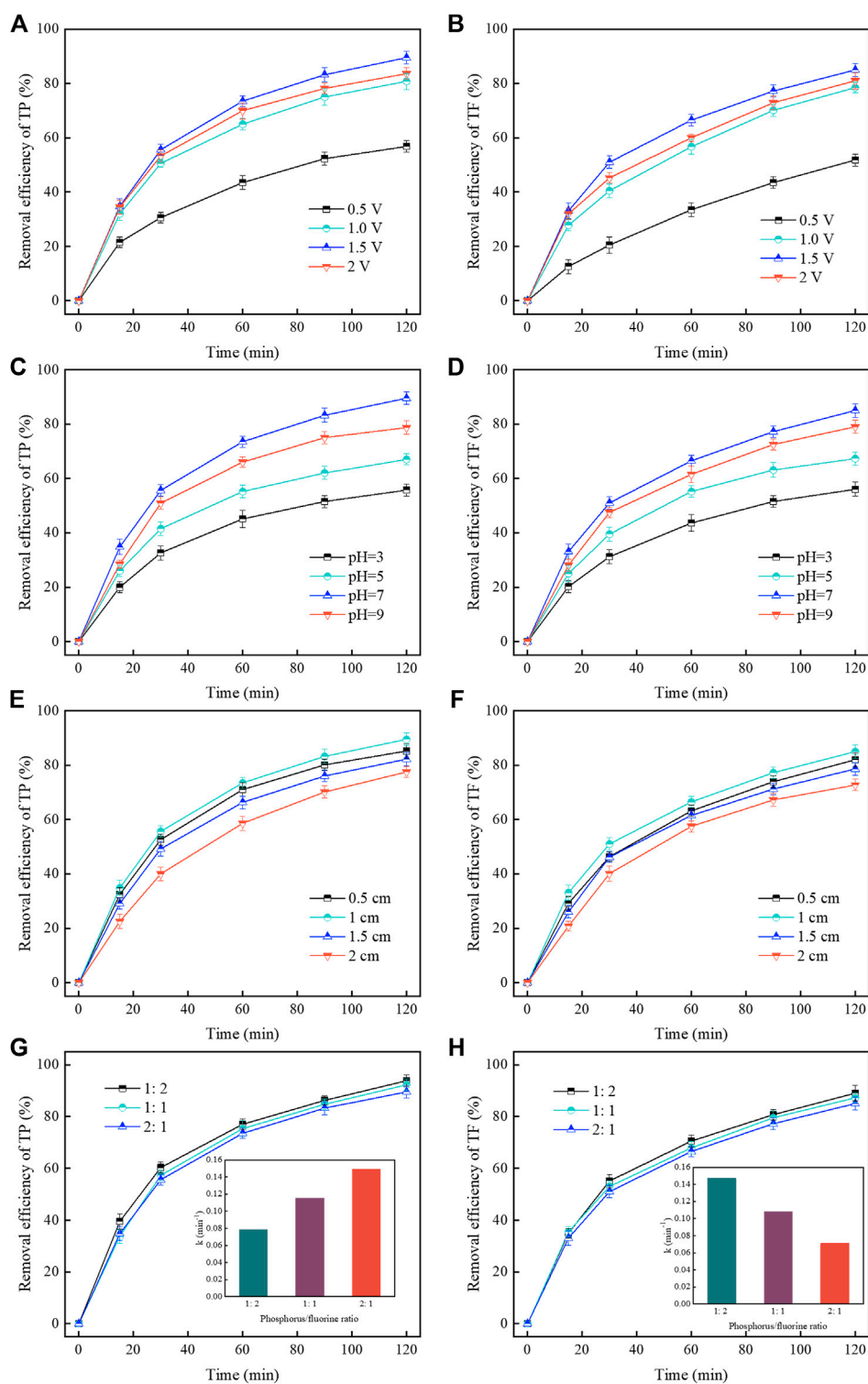


FIGURE 5

The effect of voltage intensity on removal efficiency: (A) TP. (B) TF. The effect of pH on removal efficiency: (C) TP. (D) TF. The effect of plate spacing on removal efficiency: (E) TP. (F) TF. The effect of phosphorus/fluorine ratio on removal efficiency: (G) TP (H) TF.

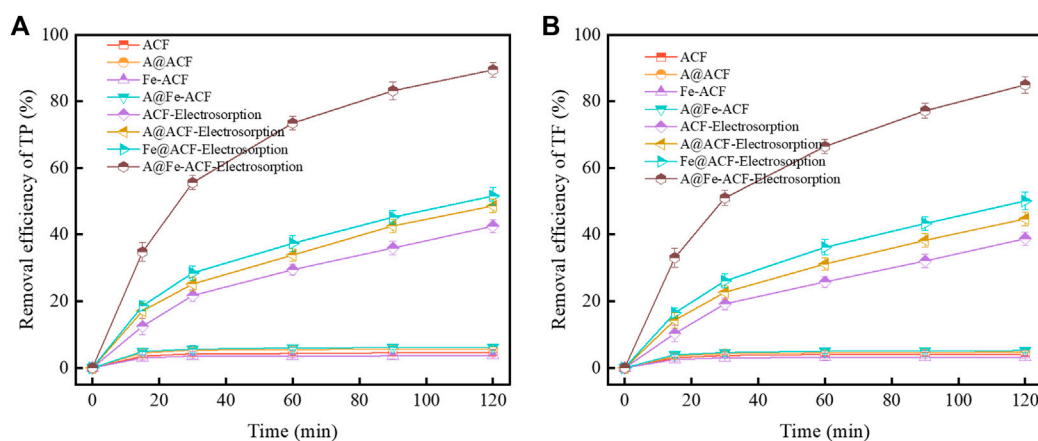


FIGURE 6
Comparison of removal efficiency under different conditions: (A) TP. (B) TF.

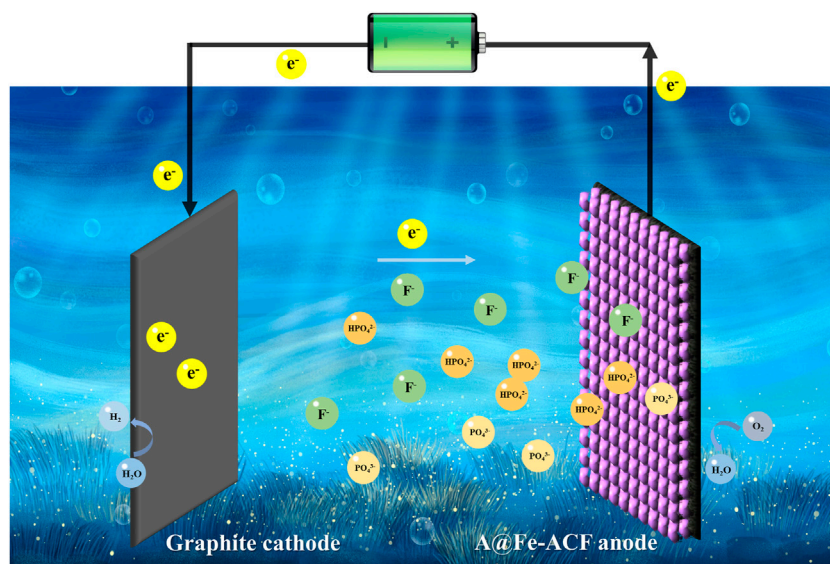
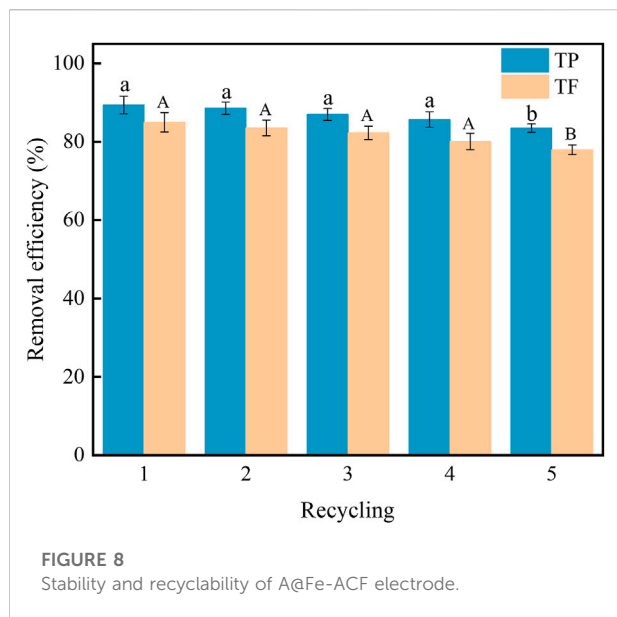


FIGURE 7
The reaction mechanism of phosphorus and fluoride removal through CDI.

side reaction Eq. 1, thus resulting in the desorption of PO_4^{3-} and F^- from the ACF and inhibiting the removal of phosphorus and fluorine (Ren et al., 2016). Therefore, 1.5 V was selected as the optimum voltage intensity. The solution pH is one of the essential factors to be considered in the removal of phosphorus and fluoride. Within a certain range, the removal efficiencies of TP and TF increased with the pH and reached the best at pH 7 (Figures 5C, D). The pH value significantly affects the existence of phosphate and fluoride ions in the solution Eqs. 2–4. When the pH is acidic, the uncharged H_3PO_4 occupies the dominant

position, while when the pH is 7, the charged HPO_4^{2-} increases (Huang et al., 2017a), then the hydration radius decreases, which is easier to be absorbed by the electric field (Gabelich et al., 2002; Huang et al., 2013). Moreover, fluorine mainly exists in the F^- when the pH is more than 6, which benefits CDI treatment and stabilization, and a good electrostatic interaction under neutral conditions can positively influence the adsorption of F^- (Martinez-Vargas et al., 2021). However, when the pH was higher than 7, the removal rate of TP and TF decreased instead. This trend may be attributed to the

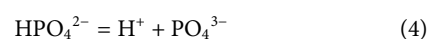
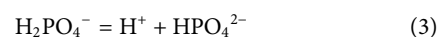


enhanced competition between phosphate ions and hydroxyl ions for electrode adsorption sites at higher pH (Huang et al., 2013). A higher pH environment could cause electrostatic repulsion to re-release the adsorbed fluoride, thus reducing the removal efficiency (Yu et al., 2018). In conclusion, pH seven would be more suitable for A@Fe-ACF electrode CDI treatment of phosphorus-fluoride wastewater. It can be seen from Figures 5E, F that the removal efficiency of TP and TF was the highest when the plate spacing is 1 cm. The closer plate spacing improved the rate of ion migration between the plates, enhanced the ions enriched on the electric double layer and the thickness of the electric double layer, further reduced the migration distance of HPO_4^{2-} and F^- in the electric field, and accelerated the adsorption of target ions. An excessively close plate spacing would interfere with the reactions between cathode and anode, and the rapidly increasing current intensity may lead to side reactions (Chai et al., 2020). In contrast, the long distance in the CDI reaction could limit ion mobility and exacerbate energy consumption (Yang et al., 2020). Therefore, 1 cm was determined as the optimal plate spacing.

Exploring the effect of the P/F ratio in wastewater on the CDI is important. The removal of TF increased with decrease in the relative concentration of phosphorus (Figures 5G, H). The adsorption rate constant of TP decreased from 0.1492 to 0.0782, while that of TF increased from 0.071 to 0.147 when the P/F ratio changed from 2:1 to 1:2. For HPO_4^{2-} , the value of Z/r (charge/radius) is higher than that of F^- , which is beneficial to its adsorption and binding on ACF (Zuo et al., 2016). When the phosphorus concentration decreased, the binding competitiveness reduced, and the adsorption trend of F^- increased. Therefore, the control of the P/F ratio in

wastewater could be a pivotal step to further improving the simultaneous treatment efficiency.

By studying the adsorption process of the coexistence of NO_3^- , Cl^- , SO_4^{2-} , HCO_3^- , and SiO_3^{2-} , it can be found that different anions concentrations have different effects on the TP and TF removal efficiency (Supplementary Figures S4A, 4B). The presence of NO_3^- and Cl^- did not affect the removal of phosphorus and fluoride significantly, while the coexistence of SO_4^{2-} , HCO_3^- , and SiO_3^{2-} had certain effect on the adsorption capacity. That could be attributed to the adsorption competition between coexisting ions with F^- and HPO_4^{2-} (Yu et al., 2018). These anions will lead to the precipitation of Ca^{2+} in the wastewater, blocking the pores of the ACF and passivating the electrodes, thereby reducing the adsorption capacity of the reaction system (Yoosefian et al., 2017). Results indicated that A@Fe-ACF can still maintain high adsorption efficiency in the presence of different ion concentrations, showing relatively excellent anti-interference performance.



3.3 Adsorption mechanism

The removal efficiency of phosphorus and fluoride under different modified conditions is shown in Figures 6A, B, including the two cases of non-electric adsorption and CDI. It could be observed that under pure adsorption conditions, acid modification and iron impregnation slightly enhanced the adsorption of TP and TF. The removal efficiency of phosphorus and fluoride increased rapidly when the electric field was applied. The increase in the specific surface area caused by the etching of pores using HNO_3 and the presence of Fe oxides provide more adsorption sites for ACF, so the acid modification assisted Fe loading significantly promoted the CDI efficiency. The adsorption kinetics of the A@Fe-ACF electrode CDI process was further investigated (Supplementary Figures S5A, 5B). The precision of the pseudo-second-order kinetic equation is better than that of the pseudo-first-order kinetics, indicating that chemical adsorption played a dominant role in this process.

The possible reaction mechanism of simultaneous phosphorus and fluoride wastewater treatment based on A@Fe-ACF electrode CDI is shown in Figure 7. Anions such as HPO_4^{2-} and F^- would move towards the anode under the action of the electric field and subsequently adsorbed on A@Fe-ACF superior. Meanwhile, the loading of Fe can promote the

TABLE 1 Comparison between the different processes.

Process	Initial properties	Parameters	Removal performance	References
Electrosorption (A@Fe-ACF)	pH 3.53, 118.2 mg/L TP, 85.7 mg/L TF	Voltage intensity 1.5 V, pH 7, plate spacing 1 cm	89.4% of TP, 85% of TF	This work
Lime process	pH 2.7, 46 mg/L PO ₄ ³⁻ 148 mg/L F ⁻	CaO as calcium source, pH 8	63%–73% of PO ₄ ³⁻ , 1%–4% of F ⁻	Grzmil and Wronkowski, (2006)
Lime process	pH 0.78, 4.58% PO ₄ ³⁻ , 5.67% TF	Ca(OH) ₂ as calcium source, 160–180 g/L, pH 2	60% of H ₃ PO ₄ , about 100% of TF	Al-Harashsheh et al. (2014)
Lime process	200 g/L phosphogypsum	1% lime of the mass of phosphogypsum	Only 0.71 mg/L of soluble phosphorus and 0.041 mg/L of soluble fluorine	Wang et al. (2020)
Magnesium salt precipitation	pH 7.5 ± 0.05, 1,280 ± 56 mg/L F ⁻ , 201 ± 3.4 mg/L PO ₄ -P	Natural brucite as magnesium source, 4 g/L brucite, pH 9.5, 240 min	97% of PO ₄ -P, 91% of F ⁻	Huang et al. (2017a)
Lanthanum salt precipitation	4.92 mg/L P, 1.26 mg/L F	pH 1–4; pH 5–11, 0.03 mol/L La ³⁺	96% of phosphate, 91.3% of fluoride	Xia et al. (2021)
Adsorption	50 mg/L P, 50 mg/L F	La@MgAl nanocomposites, 0.1 g dosage, pH 6.0 ± 0.1	95.1% of P, 55.3% of F	Kong et al. (2019)
Adsorption	10 mg/L phosphate, 15 mg/L fluoride	Carboxylated chitosan/Fe ₃ O ₄ , pH 3, 2 g/L dosage, 60 min	1.8675 mg/g phosphate, 1.2187 mg/g fluoride	Mohammadi et al. (2019)
Constructed wetland	pH 7.35, 1.29 mg/L TP, 1.44 mg/L F ⁻	18–43.6 cm/d hydraulic loading rates, 1.04–2.51 days hydraulic retention times	58%–39% of TP and TF	Wu et al. (2017)

complexation of HPO₄²⁻ and F⁻, and enhance the immobilization of pollutants on the electrodes.

3.4 Recycling and stable test

The recycling ability of the electrode is important for evaluating its stability during the CDI process. It can be seen from Figure 8 that after five cycles of A@Fe-ACF by adsorption-desorption, the removal efficiencies of TP and TF dropped to 83% and 77.6%, which still keep a good adsorption performance. The above results show that A@Fe-ACF has good stability in phosphorus-fluoride wastewater treatment.

3.5 Comparison with traditional strategies

Gradual removal of phosphate and fluoride from wastewater using precipitation was the most widely reported strategy (Table 1). After pH adjustment, phosphate and fluoride might precipitate in the form of CaHPO₄, Ca₃(PO₄)₂, and CaF₂ (Grzmil and Wronkowski, 2006). However, the dosing of large amounts of neutralizing reagents required for higher pH and the adjustment of effluent pH can be costly and operationally burden (Xia et al., 2021). A large number of generated precipitates cannot be recovered entirely, and there is a risk of secondary pollution. Some new phosphorus and fluorine treatment technologies have been proposed and achieved certain results, but the longer treatment period and lower

treatment efficiency are still enormous challenges (Wu et al., 2017; Yang et al., 2021). Efficient simultaneous removal of phosphate and fluoride from wastewater can be achieved by CDI using A@Fe-ACF. The presence of salt ions in wastewater could act as an electrolyte to improve the current efficiency, and the lower energy consumption and shorter reaction time will reduce the treatment cost. Based on the above advantages, the simultaneous removal of phosphorus and fluoride wastewater by CDI using an A@Fe-ACF electrode can be an innovative and feasible technology.

4 Conclusion

The A@Fe-ACF-400 electrode was prepared to simultaneously remove phosphorus and fluorine in wastewater by CDI. The removal of TP and TF could reach 89.4% and 85% with the optimal reaction conditions. The combined modification of acid treatment and iron loading enhanced the CDI performance using ACF while endow A@Fe-ACF-400 with good stability and recycling ability. In conclusion, A@Fe-ACF electrode CDI demonstrated promising prospects in the simultaneous treatment of phosphorus and fluoride wastewater.

Data availability statement

The original contributions presented in the study are included in the article/Supplementary Material, further inquiries can be directed to the corresponding author.

Author contributions

ZD wrote the first draft of the manuscript, organized the database, and performed the statistical analysis. TQ contributed to conception and design of the study. CB performed the statistical analysis. ZW checked the English grammar of the manuscript. YG checked the format of the manuscript. PQ contributed to conception and design of the study and provide funding supporting. All authors contributed to manuscript revision, read, and approved the submitted version.

Funding

This work was jointly supported by the Science and Technology Achievement Transformation and Industrialization Plan of Hunan Province (2020NK2001), funder: PQ, the National Natural Science Foundation of China (No. 51808215), funder: ZW, the Hunan Provincial Natural Science Foundation of China (2019JJ50253), funder: ZW.

References

- Al-Harashsheh, M., Batiha, M., Kraishan, S., and Al-Zoubi, H. (2014). Precipitation treatment of effluent acidic wastewater from phosphate-containing fertilizer industry: Characterization of solid and liquid products. *Sep. Purif. Technol.* 123, 190–199. doi:10.1016/j.seppur.2013.12.027
- Ayranci, E., and Conway, B. E. (2001). Adsorption and electrosorption at high-area carbon-felt electrodes for waste-water purification: Systems evaluation with inorganic, S-containing anions. *J. Appl. Electrochem.* 31, 257–266. doi:10.1023/A:1017528002713
- Chai, Y., Qin, P., Wu, Z., Bai, M., Li, W., Pan, J., et al. (2021). A coupled system of flow-through electro-Fenton and electrosorption processes for the efficient treatment of high-salinity organic wastewater. *Sep. Purif. Technol.* 267, 118683. doi:10.1016/j.seppur.2021.118683
- Chai, Y., Qin, P., Zhang, J., Li, T., Dai, Z., and Wu, Z. (2020). Simultaneous removal of Fe(II) and Mn(II) from acid mine wastewater by electro-Fenton process. *Process Saf. Environ. Prot.* 143, 76–90. doi:10.1016/j.psep.2020.06.026
- Chen, Z., Zhang, H., Wu, C., Wang, Y., and Li, W. (2015). A study of electrosorption selectivity of anions by activated carbon electrodes in capacitive deionization. *Desalination* 369, 46–50. doi:10.1016/j.desal.2015.04.022
- Foo, K. Y., and Hameed, B. H. (2009). A short review of activated carbon assisted electrosorption process: An overview, current stage and future prospects. *J. Hazard. Mat.* 170 (2–3), 552–559. doi:10.1016/j.jhazmat.2009.05.057
- Gabelich, C. J., Tran, T. D., and Suffet, I. H. (2002). Electrosorption of inorganic salts from aqueous solution using carbon aerogels. *Environ. Sci. Technol.* 36, 3010–3019. doi:10.1021/es0112745
- Gaikwad, M. S., and Balomajumder, C. (2017). Tea waste biomass activated carbon electrode for simultaneous removal of Cr(VI) and fluoride by capacitive deionization. *Chemosphere* 184, 1141–1149. doi:10.1016/j.chemosphere.2017.06.074
- Georgakopoulos, A. (2003). Study of low rank Greek coals using FTIR spectroscopy. *Energy sources*. 25 (10), 995–1005. doi:10.1080/00908310390232442
- Gouider, M., Feki, M., and Sayadi, S. (2010). Bioassay and use in irrigation of untreated and treated wastewaters from phosphate fertilizer industry. *Ecotoxicol. Environ. Saf.* 73 (5), 932–938. doi:10.1016/j.ecoenv.2009.12.021
- Grzmil, B., and Wronkowski, J. (2006). Removal of phosphates and fluorides from industrial wastewater. *Desalination* 189 (1–3), 261–268. doi:10.1016/j.desal.2005.07.008

Conflict of interest

The authors declare that the research was conducted in the absence of any commercial or financial relationships that could be construed as a potential conflict of interest.

Publisher's note

All claims expressed in this article are solely those of the authors and do not necessarily represent those of their affiliated organizations, or those of the publisher, the editors and the reviewers. Any product that may be evaluated in this article, or claim that may be made by its manufacturer, is not guaranteed or endorsed by the publisher.

Supplementary material

The Supplementary Material for this article can be found online at: <https://www.frontiersin.org/articles/10.3389/fenvs.2022.1087231/full#supplementary-material>

- Huang, G. H., Chen, T. C., Hsu, S.-F., Huang, Y. H., and Chuang, S. H. (2013). Capacitive deionization (CDI) for removal of phosphate from aqueous solution. *Desalination Water Treat.* 52 (4–6), 759–765. doi:10.1080/19443994.2013.826331
- Huang, H., Liu, J., Zhang, P., Zhang, D., and Gao, F. (2017a). Investigation on the simultaneous removal of fluoride, ammonia nitrogen and phosphate from semiconductor wastewater using chemical precipitation. *Chem. Eng. J.* 307, 696–706. doi:10.1016/j.cej.2016.08.134
- Huang, X., He, D., Tang, W., Kovalsky, P., and Waite, T. D. (2017b). Investigation of pH-dependent phosphate removal from wastewaters by membrane capacitive deionization (MCDI). *Environ. Sci. Water Res. Technol.* 3 (5), 875–882. doi:10.1039/c7ew00138j
- Kalfa, A., Shapira, B., Shopin, A., Cohen, I., Avraham, E., and Aurbach, D. (2020). Capacitive deionization for wastewater treatment: Opportunities and challenges. *Chemosphere* 241, 125003. doi:10.1016/j.chemosphere.2019.125003
- Kong, L., Tian, Y., Pang, Z., Huang, X., Li, M., Yang, R., et al. (2019). Synchronous phosphate and fluoride removal from water by 3D rice-like lanthanum-doped La/MgAl nanocomposites. *Chem. Eng. J.* 371, 893–902. doi:10.1016/j.cej.2019.04.116
- Lin, S., Yang, X., Liu, L., Li, A., and Qiu, G. (2022). Electrosorption of cadmium and arsenic from wastewaters using nitrogen-doped biochar: Mechanism and application. *J. Environ. Manage.* 301, 113921. doi:10.1016/j.jenvman.2021.113921
- Martinez-Vargas, D. R., Larios-Durán, E. R., Chazaro-Ruiz, L. F., and Rangel-Mendez, J. R. (2021). Correlation between physicochemical and electrochemical properties of an activated carbon doped with lanthanum for fluoride electrosorption. *Sep. Purif. Technol.* 268, 118702. doi:10.1016/j.seppur.2021.118702
- Meng, N., Ren, J., Liu, Y., Huang, Y., Petit, T., and Zhang, B. (2018). Engineering oxygen-containing and amino groups into two-dimensional atomically-thin porous polymeric carbon nitrogen for enhanced photocatalytic hydrogen production. *Energy Environ. Sci.* 11 (3), 566–571. doi:10.1039/c7ee03592f
- Mohammadi, E., Daraei, H., Ghanbari, R., Dehestani Athar, S., Zandsalimi, Y., Ziaee, A., et al. (2019). Synthesis of carboxylated chitosan modified with ferromagnetic nanoparticles for adsorptive removal of fluoride, nitrate, and phosphate anions from aqueous solutions. *J. Mol. Liq.* 273, 116–124. doi:10.1016/j.molliq.2018.10.019
- Ren, G., Zhou, M., Liu, M., Ma, L., and Yang, H. (2016). A novel vertical-flow electro-Fenton reactor for organic wastewater treatment. *Chem. Eng. J.* 298, 55–67. doi:10.1016/j.cej.2016.04.011

- Ren, S., Usman, M., Tsang, D. C. W., S. O. T., Angelidaki, I., Zhu, X., et al. (2020). Hydrochar-facilitated anaerobic digestion: Evidence for direct interspecies electron transfer mediated through surface oxygen-containing functional groups. *Environ. Sci. Technol.* 54 (9), 5755–5766. doi:10.1021/acs.est.0c00112
- Song, X., Liu, J., Jiang, Q., Zhang, P., Shao, Y., He, W., et al. (2019). Enhanced electron transfer and methane production from low-strength wastewater using a new granular activated carbon modified with nano-Fe₃O₄. *Chem. Eng. J.* 374, 1344–1352. doi:10.1016/j.cej.2019.05.216
- Verma, R., Chauhan, A., NehaBattoo, K. M., Kumar, R., Hadhi, M., Raslan, E. H., et al. (2021). Effect of calcination temperature on structural and morphological properties of bismuth ferrite nanoparticles. *Ceram. Int.* 47 (3), 3680–3691. doi:10.1016/j.ceramint.2020.09.220
- Wang, F. C., Feve, M., Lam, T. M., and Pascault, J.-P. (1994). FTIR analysis of hydrogen bonding in amorphous linear aromatic polyurethanes. I. Influence of temperature. *J. Polym. Sci. B. Polym. Phys.* 32 (8), 1305–1313. doi:10.1002/polb.1994.090320801
- Wang, J., Dong, F., Wang, Z., Yang, F., Du, M., Fu, K., et al. (2020). A novel method for purification of phosphogypsum. *Physicochem. Probl. Min. Process.* 56 (5), 975–983. doi:10.37190/ppmp/127854
- Wang, R., Liu, H., Zhang, K., Zhang, G., Lan, H., and Qu, J. (2021). Ni(II)/Ni(III) redox couple endows Ni foam-supported Ni₂P with excellent capability for direct ammonia oxidation. *Chem. Eng. J.* 404, 126795. doi:10.1016/j.cej.2020.126795
- Wu, T., Wang, G., Dong, Q., Qian, B., Meng, Y., and Qiu, J. (2015). Asymmetric capacitive deionization utilizing nitric acid treated activated carbon fiber as the cathode. *Electrochimica Acta* 176, 426–433. doi:10.1016/j.electacta.2015.07.037
- Wu, Y., Han, R., Yang, X., Zhang, Y., and Zhang, R. (2017). Long-term performance of an integrated constructed wetland for advanced treatment of mixed wastewater. *Ecol. Eng.* 99, 91–98. doi:10.1016/j.ecoleng.2016.11.032
- Xia, L., Zhang, W., Che, J., Chen, J., Wen, P., Ma, B., et al. (2021). Stepwise removal and recovery of phosphate and fluoride from wastewater via pH-dependent precipitation: Thermodynamics, experiment and mechanism investigation. *J. Clean. Prod.* 320, 128872. doi:10.1016/j.jclepro.2021.128872
- Yang, H., Fu, P., Zhang, G., Zhang, Q., and Li, X. (2021). Adsorption removal of phosphate and fluoride from aqueous solution using oily sludge-based pyrolysis residue. *Environ. Process.* 8 (4), 1517–1531. doi:10.1007/s40710-021-00539-7
- Yang, Z., Chen, H., Wang, J., Yuan, R., Wang, F., and Zhou, B. (2020). Efficient degradation of diisobutyl phthalate in aqueous solution through electro-Fenton process with sacrificial anode. *J. Environ. Chem. Eng.* 8 (5), 104057. doi:10.1016/j.jece.2020.104057
- Yoosefian, M., Ahmadzadeh, S., Aghasi, M., and Dolatabadi, M. (2017). Optimization of electrocoagulation process for efficient removal of ciprofloxacin antibiotic using iron electrode; kinetic and isotherm studies of adsorption. *J. Mol. Liq.* 225, 544–553. doi:10.1016/j.molliq.2016.11.093
- Yu, Z., Xu, C., Yuan, K., Gan, X., Feng, C., Wang, X., et al. (2018). Characterization and adsorption mechanism of ZrO₂ mesoporous fibers for health-hazardous fluoride removal. *J. Hazard. Mat.* 346, 82–92. doi:10.1016/j.jhazmat.2017.12.024
- Zhang, J., Tang, L., Tang, W., Zhong, Y., Luo, K., Duan, M., et al. (2020). Removal and recovery of phosphorus from low-strength wastewaters by flow-electrode capacitive deionization. *Sep. Purif. Technol.* 237, 116322. doi:10.1016/j.seppur.2019.116322
- Zuo, Y., Fu, X., Chen, Y., Cui, G., and Liu, M. (2016). Phosphorus removal from wastewater using a lanthanum oxide-loaded ceramic adsorbent. *Adsorption* 22 (8), 1091–1098. doi:10.1007/s10450-016-9831-8